

RECOGNITION OF PICK WEAR CONDITION BASED ON GREY-MARKOV CHAIN MODEL

QIANG ZHANG

*School of Mechanical Engineering, Liaoning Technical University, Liaoning, China, and
School of Mechatronics, Shandong University of Science and Technology, Shandong, China*

JIAYAO ZHANG

*School of Mechanical Engineering, Liaoning Technical University, Liaoning, China
Corresponding author J. Zhang, e-mail: 1725157910@qq.com*

An attempt is made in this paper to solve the pick wear problem of mining machinery and propose a pick wear degradation model based on the Grey-Markov chain by using generated characteristic signals and certain pick wear parameters to enhance the prediction accuracy. The vibration and acoustic emission signals generated during the catting pick are extracted and analyzed. The energy and the value of the characteristic signal are obtained by wavelet analysis to construct a characteristic sample library of the signals. Two kinds of signals are applied to the model to analyze the error between the real and the predicted values. The model prediction results demonstrate a 1.43% error of the vibration signal, 1.64% error of the acoustic emission signal with 98% prediction accuracy, thus offers a new method for monitoring the pick wear of mining machinery.

Keywords: pick wear, vibration acceleration signal, acoustic emission signal, Grey-Markov method

1. Introduction

The pick is one of the most important parts of mining machinery. Currently, the condition of coal quality is worsening day by day. The coal, rock and hard rock are in contact with each other over a prolonged period under a state of high impact and stress, thereby, damaging and shortening the life of the pick severely and warranting replacements of coal mining machinery parts. Therefore, the pick wear has become one of the main research problems in the coal mining (Bagri *et al.*, 2021; Boing *et al.*, 2020; Chen *et al.*, 2020; Fan *et al.*, 2020).

Several common signal-based wear methods are advocated by scholars to reduce the catting pick wear problem including the characteristic parameter method, time series analysis, and Fourier transform (Hu *et al.* 2019; Lan *et al.*, 2020; Li *et al.*, 2020). The signal quantity recorded by the characteristic parameter method is large, and the real-time analysis is strong. However, the connection between the acoustic emission waveform obtained and the acoustic emission source mechanism must be understood while using this method, otherwise the physical nature of the acoustic emission waveform cannot be found. Although the application of time series analysis in some cases have achieved some results, this method cannot explain the reason of calculating the auto-regressive coefficient and three catting pick factors as input variables of a neural network (Lubis *et al.*, 2020; Ma *et al.*, 2020). Fourier transformation embodies information of the signal in the frequency domain and does not change with time. For the wear method, it is common to study the wear condition between a metal and metal. Abaqus software and a dynamic model can accurately predict the wear condition. Similarly, these theoretical methods are also applicable to pick wear. (Shen *et al.*, 2020; Ouafik, 2020; Shadfar and Molatefi, 2017; Łuczak *et al.*, 2022).

In view of this, an attempt is made to adopt the Grey-Markov model prediction method based on the identification of pick wear degree of the vibration signal and the acoustic emission signal. The method is characterized by a small stable error in the calculation process by dividing the state parameters. The precise prediction of pick wear is realized by extracting a variety of feature information related to the pick wear state by analyzing and processing.

2. Online monitoring system for pick wear characteristic signals

2.1. Establishment of an experimental system for pick wear monitoring

The experimental system mainly consists of two parts: the pick and the multi-sensor testing subsystem. The pick consists of the pick mechanism, walking mechanism and control cabinet. The multi-sensor test system consists of the vibration signal acquisition system, acoustic emission signal acquisition system and current signal acquisition system. Its main form of composition is shown in Fig. 1.

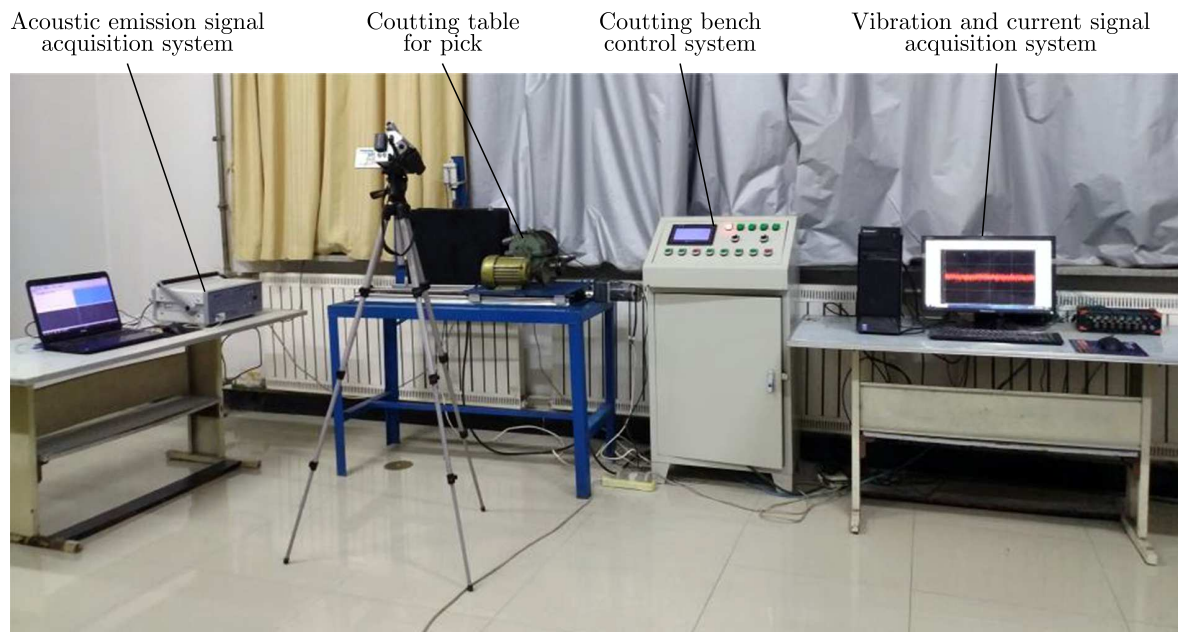


Fig. 1. Pick wear monitoring experimental system

2.2. Monitoring signal extraction

The pick wear can be divided into 6 states, namely, new pick, slight wear, medium wear, large wear, severe wear and failure pick (A1-A6), respectively.

2.2.1. Vibration signal extraction

The vibration signals in the pick process are collected, and the signal characteristics are analyzed to judge the wear degree of the picking gear. The vibration acceleration curves of X -axis in the pick process for different wear degrees are selected as characteristic signals. The vibration acceleration signals measured in picks with different wear degrees are shown in Fig. 2a-2f displaying vibration acceleration curves in X -axis direction.

It can be seen from Fig. 2 that with deterioration of the pick wear degree, the pick vibration is continuously intensified, and the vibration acceleration average peak of pick is steadily increasing.

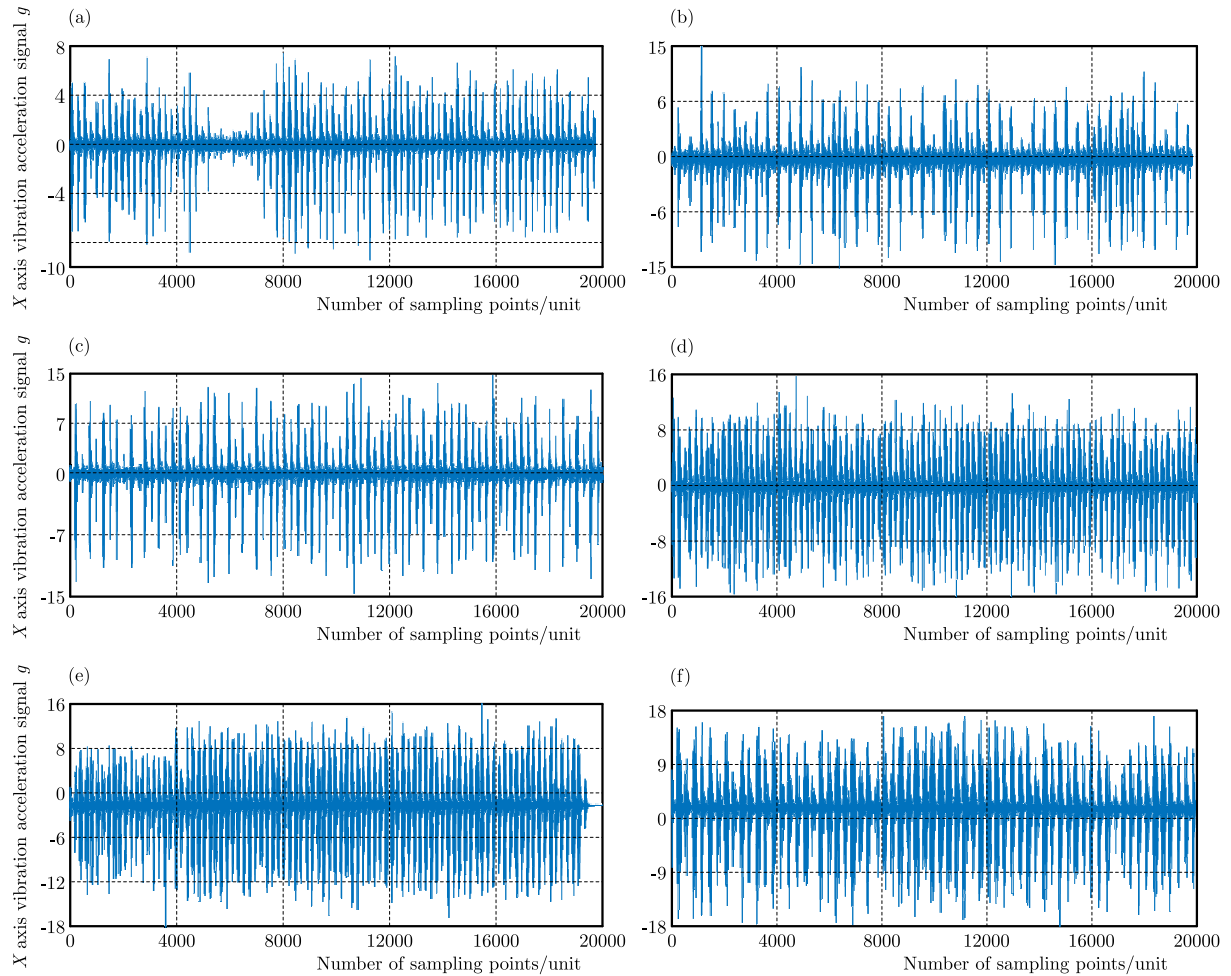


Fig. 2. X -axis vibration acceleration curves for different wear degrees: (a) new pick, (b) slight wear, (c) medium wear, (d) large wear, (e) severe wear, (f) failure pick

The average peak acceleration is 3.98 g, 4.52 g, 5.49 g, 6.51 g, 8.52 g and 9.52 g, respectively. The pick vibration acceleration corresponding to the failure pick is the largest. Through tests and extraction of the signal, it can be noticed that with the aggravation of the pick wear degree, the average peak vibration acceleration of the pick increases continuously and the change is more obvious. Hence, a change in the vibration acceleration signal change is taken as the characteristic signal.

2.2.2. Acoustic emission signal extraction

The frequency of the acoustic emission signal is high. Collisions, friction and plastic deformations in the pick process result in outward propagation of the energy and sound waves. According to the difference of acoustic emission signals in the pick process between picks with different wear degrees and coal rock, the wear degree can be determined as depicted in Fig. 3.

According to Fig. 3a-3f, with a change in the picking gear wear degree, the peak values of the acoustic emission signals correspond to 5.034 V, 3.94 V, 2.85 V, 1.44 V, 0.62 V and 0.43 V, respectively. Through testing and extraction, it can be seen that with the aggravation of picking gear wear, the acoustic emission signal gradually decreases, a change in the pick acoustic emission signal is obvious, and the amplitude fluctuates greatly, so the change of the acoustic emission signal of the picking gear is taken as the characteristic signal.

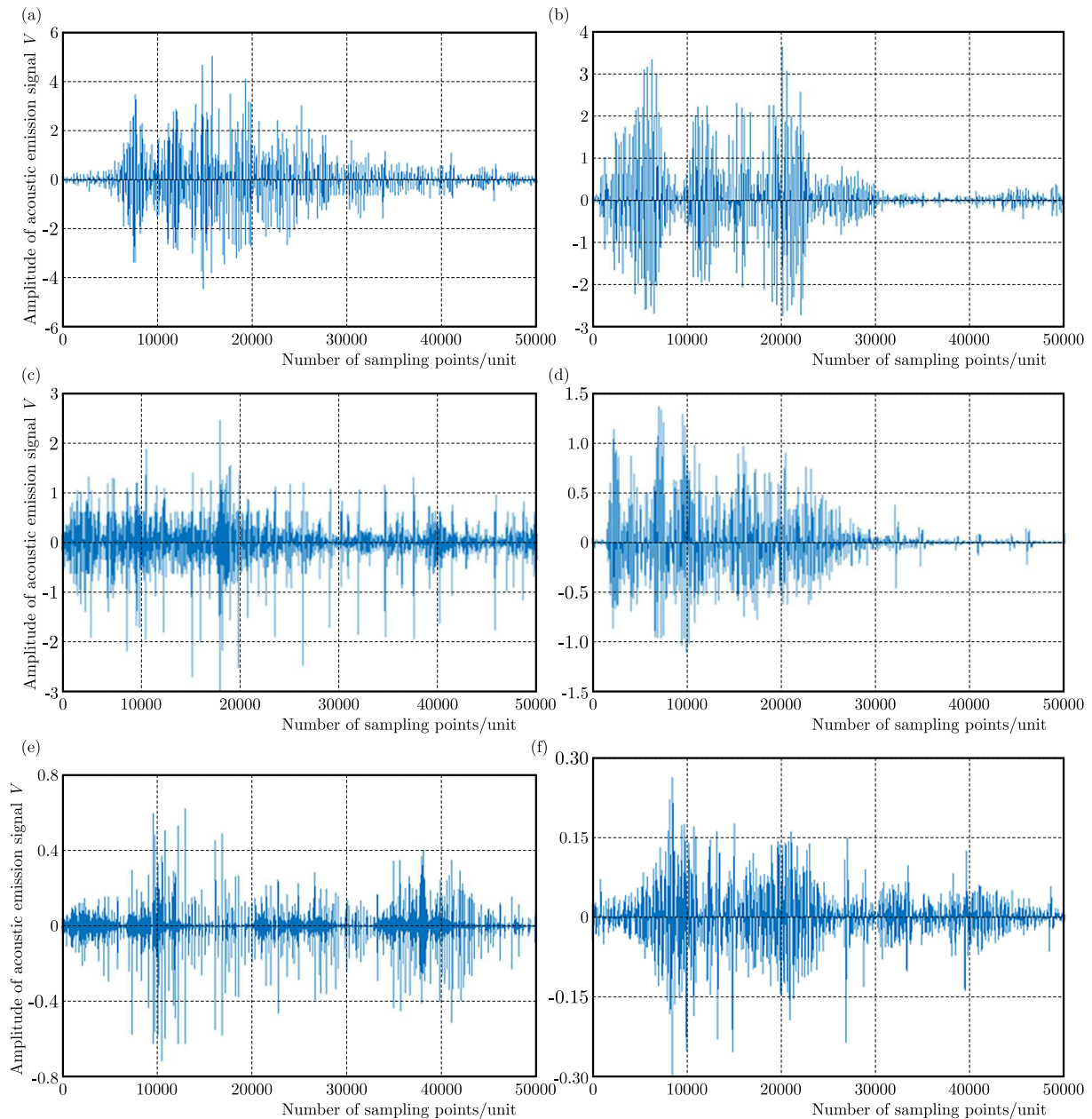


Fig. 3. X -axis acoustic emission acceleration curves for different wear degrees: (a) new pick, (b) slight wear, (c) medium wear, (d) large wear, (e) severe wear, (f) failure pick

2.3. Analysis and recognition of characteristic signals

2.3.1. Wavelet packet analysis of vibration signal

Three-layer wavelet packet decomposition is used to decompose vibration acceleration time domain signals of the pick in six states, and the signals are decomposed into eight frequency bands. After the signal decomposition, each node is de-noised as (3.0), (3.1), (3.2), (3.3), (3.4), (3.5), (3.6), and (3.7). The frequency band range of each node after the signal decomposition is shown in Table 1. Figure 4 depicts the wavelet packet decomposition diagram of each state (part of the picture). The abscissa is the number of sampling points in each frequency band, and the ordinate is the signal energy in the corresponding frequency band after the wavelet packet decomposition.

Table 1. Corresponding frequency band of each node signal

Number	Frequency [kHz]	Number	Frequency [kHz]
(3.0)	0-12.5	(3.4)	50-62.5
(3.1)	12.5-25	(3.5)	62.5-75
(3.2)	25-37.5	(3.6)	75-87.5
(3.3)	37.5-50	(3.7)	87.5-100

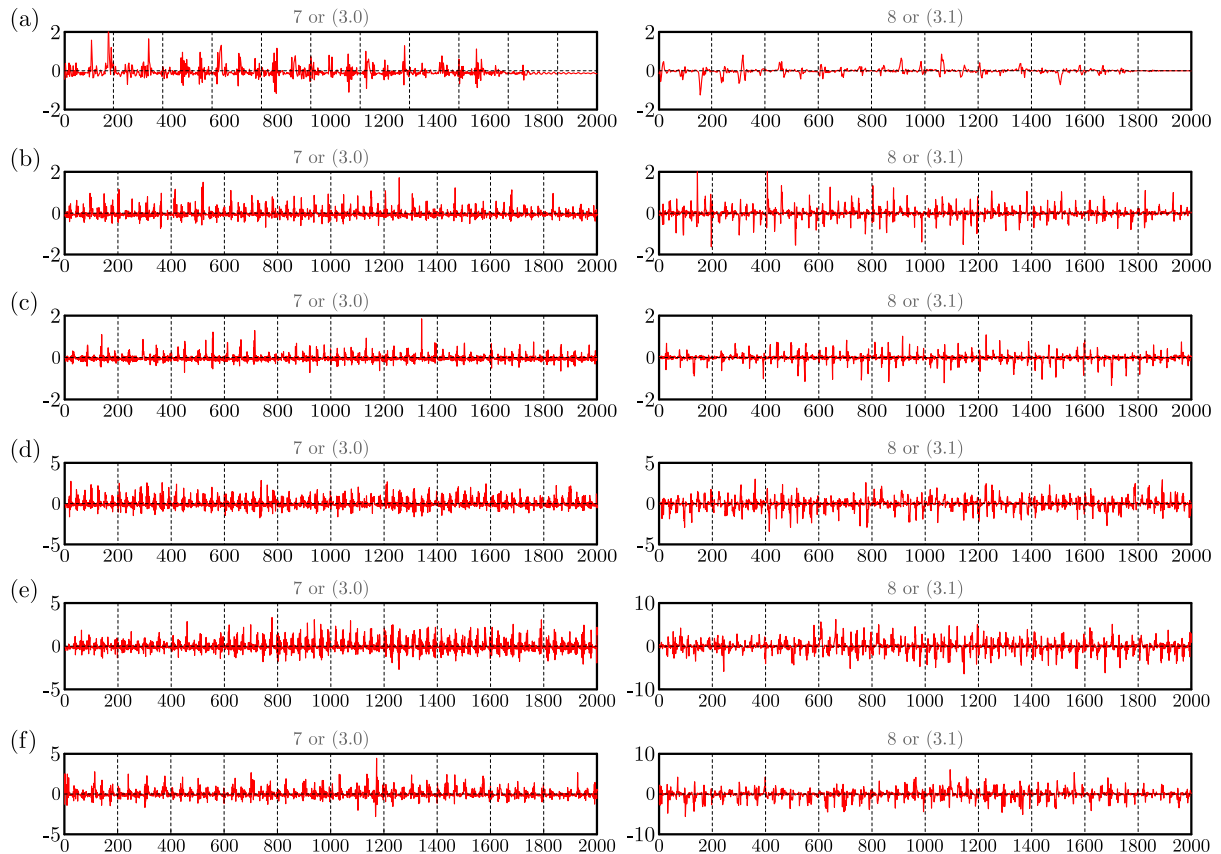


Fig. 4. Wavelet packet decomposition diagrams: (a) new pick, (b) slight wear, (c) medium wear, (d) large wear, (e) severe wear, (f) failure pick

It is evident from Fig. 4 that the signal intensity in (3.0)-(3.3) frequency band is small, whereas both the signal intensity and energy value in (3.4)-(3.7) frequency band are large with an obvious vibration amplitude. With the aggravation of the pick wear degree, the peak value and the energy value of the same frequency band also increase gradually. With deterioration of the pick wear degree, the amplitude of the vibration acceleration signal increases continuously with obvious changes, which can realize the recognition of different pick wear degrees.

The energy of each frequency band range of A1-A6 picks is calculated, and the energy values of each frequency band of 6 picks obtained with different wear degrees are shown in Fig. 5.

It is evident from Fig. 5 that the vibration energy of six picks with different wear degrees in the same frequency band exhibits a gradual increasing trend, among which the energy values in the frequency bands of 50-62.5 Hz, 62.5-75 Hz, 75-87.5 Hz and 87.5-100 Hz are higher and the change rule is obvious. Therefore, the sum of these four frequency energy bands is selected as the feature samples. Some of the data samples are shown in Table 2.

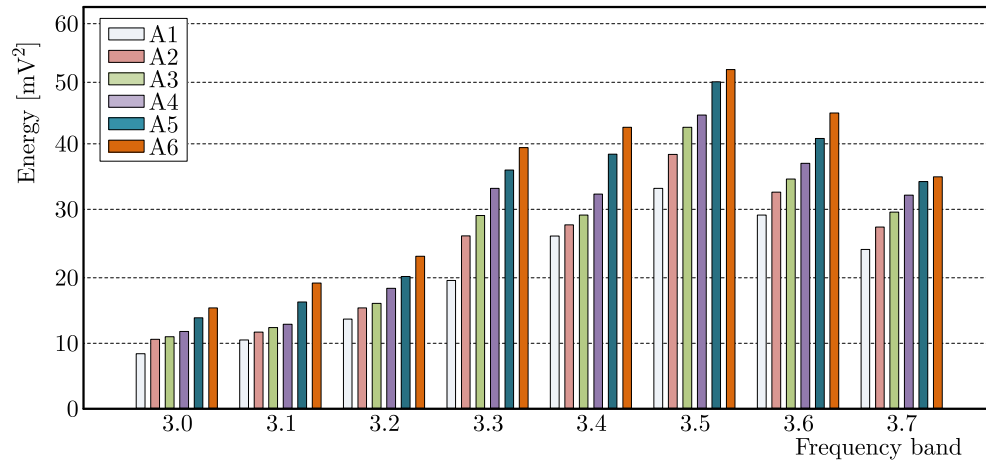


Fig. 5. Energy values of X-axis frequency band

Table 2. Sum of the energy for different pick vibration acceleration signal samples [mV²]

Number	A1	A2	A3	A4	A5	A6
1	100.0061	112.3315	126.2487	145.2145	171.9594	209.9130
2	100.7538	112.8459	126.4478	146.5461	171.1254	210.6678
⋮	⋮	⋮	⋮	⋮	⋮	⋮
49	114.6851	126.6147	147.5921	171.8481	209.1217	226.6507
50	114.9854	126.5984	147.8459	172.0114	209.1584	226.9761

2.3.2. Wavelet packet analysis of the acoustic emission signal

In line with the aforesaid vibration signals, DB9 wavelet basis is selected, and the wavelet packet decomposition of the pick in each state (part of the picture) is shown in Fig. 6. By comparing the decomposition diagrams of the eight frequency bands of A1-A6 picks, it is noticed that the signal intensity is higher in frequency band (3.1)-(3.3), the acoustic emission signal amplitude is more obvious, and the energy value is higher. The peak value and the energy value of the same frequency band increase gradually with the aggravation of pick wear.

In order to analyze the acoustic emission wavelet packet signal characteristic samples, the energy of each frequency band range of A1-A6 cutter is calculated, and the energy values of each frequency band of six cutters with different wear degrees are given. Figure 7 reveals that the vibration energy shows a trend of gradual decline. Among these, the energy values of 12.5-25 kHz, 25-37.5 kHz and 37.5-50 kHz frequency bands are relatively high and have obvious changing rules. Therefore, the energy and values of the above 3 frequency bands are selected as the feature samples. Some of the feature samples are shown in Table 3.

Table 3. Sum of the energy for different picks acoustic emission signal samples [mV²]

Number	A1	A2	A3	A4	A5	A6
1	64.5960	49.1954	38.0999	29.0012	24.5987	16.8302
2	64.5881	49.1548	38.0451	28.9445	24.5146	16.4791
⋮	⋮	⋮	⋮	⋮	⋮	⋮
49	48.8031	37.9921	28.7279	23.5145	16.8762	11.0043
50	48.7894	37.8489	28.6145	23.1547	16.6016	10.9641

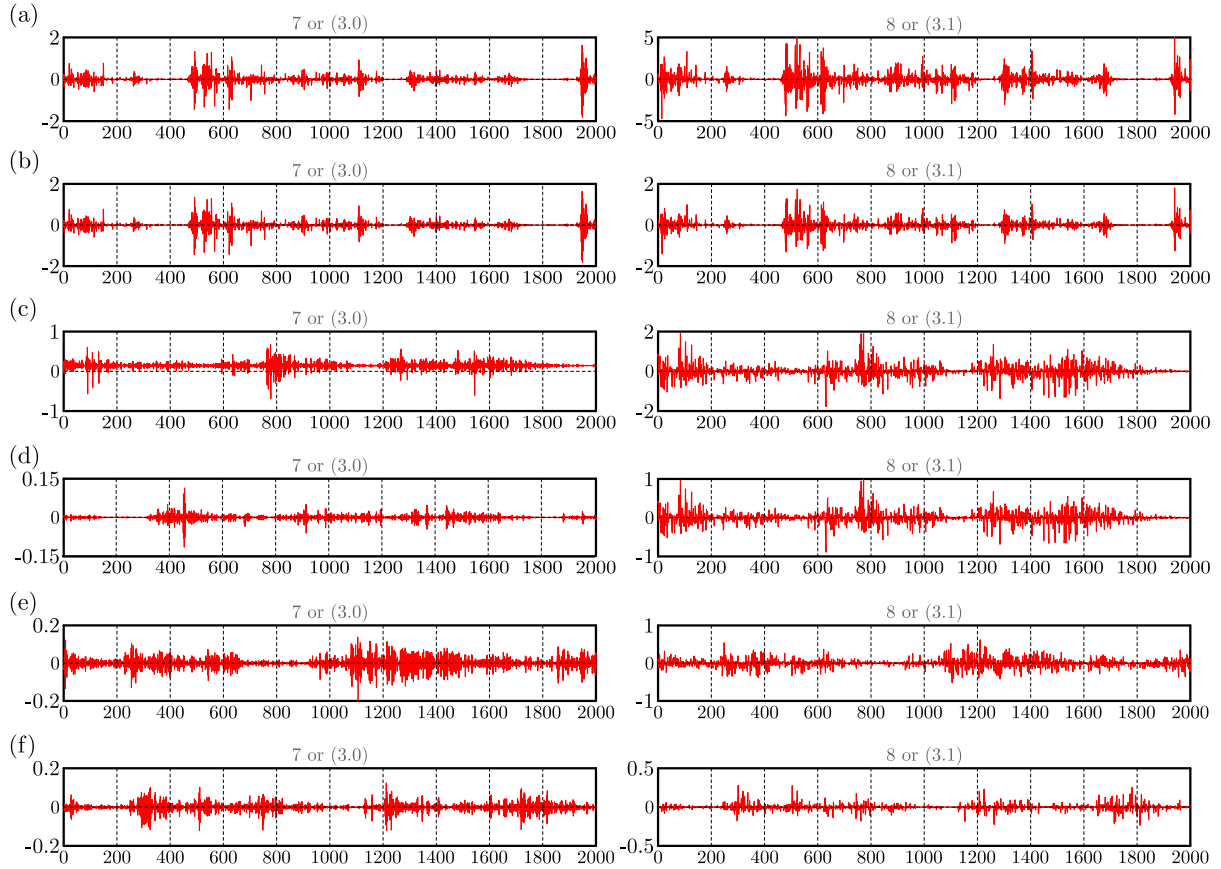


Fig. 6. Wavelet packet decomposition of different picks: (a) new pick, (b) slight wear, (c) medium wear, (d) large wear, (e) severe wear, (f) failure pick

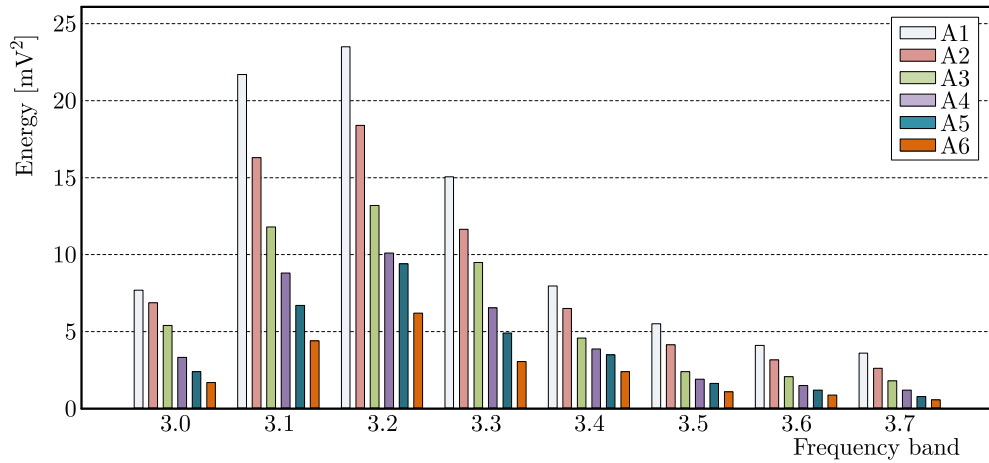


Fig. 7. Energy values of X-axis frequency band

3. Construction of the pick wear prediction model

3.1. Construction of the Grey-Markov chain model

The most basic model used in the Markov analysis is

$$\mathbf{x}(k + 1) = \mathbf{x}(k) \times \mathbf{P} \tag{3.1}$$

where $\mathbf{x}(k)$ is the state vector of the predicted object at time $t = k$. $\mathbf{x}(k + 1)$ is the state vector of the predicted object at time $t = k + 1$ and \mathbf{P} is the one-step state transition probability.

3.1.1. Partitioned prediction state

According to the predicted value of the original data, the relative value can reasonably be divided into several states with the following state interval

$$\mathbf{Q} = \frac{\mathbf{x}(t)}{\mathbf{X}(t)} \quad \mathbf{E}_i = [Q_{i1}, Q_{i2}] \quad i = 1, 2, \dots, k \quad (3.2)$$

where Q_{i1} is the upper limit of the residual value in the state interval and Q_{i2} is the lower limit of the residual value of the state interval.

3.1.2. Calculate the state transition probability matrix

After determining the state of the predicted state sequence, the original data can be divided into multiple states according to the non-stationary random use property of the Markov chain, and the expression \mathbf{E}_i of each state is given by

$$\begin{aligned} \mathbf{E}_i &= [\mathbf{E}'_{1i}, \mathbf{E}'_{2i}] & \mathbf{E}'_{1i} &\in \mathbf{E}_i & \mathbf{E}'_{1i} &= \mathbf{x}(t) + \mathbf{A}_i \\ \mathbf{E}'_{2i} &= \mathbf{x}(t) + \mathbf{B}_i & i &= 1, 2, \dots, n \end{aligned}$$

where P_{ij} is the one-step transition probability from state \mathbf{E}_i to state \mathbf{E}_j

$$P_{ij} = \frac{M_{ij}}{M_i} \quad (3.3)$$

where for $i, j = 1, 2, \dots, n$, $0 \leq P_{ij} \leq 1$, $\sum_{i=1}^n P_{ij} = 1$ and

$$\mathbf{P}(k) = \begin{bmatrix} P_{11}(k) & P_{12}(k) & \cdots & P_{1n}(k) \\ P_{21}(k) & P_{22}(k) & \cdots & P_{2n}(k) \\ \vdots & \vdots & \ddots & \vdots \\ P_{n1}(k) & P_{n2}(k) & \cdots & P_{nn}(k) \end{bmatrix}$$

3.1.3. Markov test

When

$$\hat{x}^2 = 2 \sum_{i=1}^n \sum_{j=1}^n f_{ij} \left| \frac{p_{ij}}{p_j} \right|$$

if $\hat{x} > x_{\alpha}^2 ((n-1)^2)$, then this data meets the Markov test.

3.1.4. Calculate the predicted value of the Markov model

In the state \mathbf{E}'_j , where the predicted located state sequence is determined, the predicted value of the Grey-Markov model can be obtained according to the median relative value of state $[Q_{i1} + Q_{i2}]/2$, as follows

$$y(k) = \frac{Q_{i1} + Q_{i2}}{2} + x^{(0)}(k) \quad (3.4)$$

3.2. Accuracy test of the Grey-Markov model

In order to test whether the model is qualified, the ratio of the residual error, relative error and posterior difference between the two is calculated, and each result meets the requirements of series. The accuracy test index is:

— Mean relative error

$$\bar{\Delta} = \frac{1}{n} \sum_{t=1}^n \frac{|\varepsilon(t)|}{x(t)} \cdot 100\% \quad (3.5)$$

where $\varepsilon(t)$ is the data residual sequence.

— Posterior difference ratio

$$C = \frac{S_2}{S_1} \quad (3.6)$$

where S_1 is the standard deviation of the original sequence, and S_2 is the standard deviation of the residual sequence.

— Small error probability

$$P = \{\varepsilon(t) - \bar{\varepsilon}(t)\} < 0.6745S_1 \quad (3.7)$$

where $\varepsilon(t)$ is the data residual sequence, $\bar{\varepsilon}(t)$ is the mean value of the residual sequence.

The test results are shown in Table 4.

Table 4. Model test results

Feature samples	Residual	Error probability	Posterior value ratio	Relative error
Energy and vibration signal within 50-100 Hz	22.33	1	0.013	0.0015
Energy and emission signal from 50 Hz to 100 Hz	25.53	1	0.006	0.00076

It is observed from the table that for the mean value of the residual error and the relative error of each characteristic sample, the posterior error ratio $C = S_2/S_1 < 0.35$, the error probability P is 1, which proves that the model accuracy at the first-level is good.

4. Prediction of the pick wear state based on the Grey-Markov model

4.1. Vibration signal prediction model

The energy and feature samples of the vibration acceleration signal are synthesized into feature vectors $\mathbf{x}^{(0)}$

$$\mathbf{x}^{(1)} = [100.00, 100.75, 101.64, 102.19, \dots, 226.00, 226.33, 226.65, 226.98]$$

The matrix \mathbf{B} and vector \mathbf{Y}_n are obtained according to the Grey-Markov rule as follows

$$\mathbf{B} = \begin{bmatrix} -100.3750 & 1 \\ -101.1950 & 1 \\ -101.9150 & 1 \\ -102.3700 & 1 \\ \vdots & \vdots \\ -225.8372 & 1 \\ -226.1626 & 1 \\ -226.4880 & 1 \\ -226.8134 & 1 \end{bmatrix}$$

$$\mathbf{Y}_n = [100.75, 101.64, 102.19, 102.55, \dots, 226.00, 226.33, 226.65, 226.98]$$

$$\mathbf{x} = \begin{bmatrix} a \\ u \end{bmatrix} = (\mathbf{B}^T \mathbf{B})^{-1} \mathbf{B}^T \mathbf{Y} = \begin{bmatrix} -0.0030 \\ 95.8188 \end{bmatrix}$$

The solution

$$\hat{x}^{(1)}(t+1) = \left(100.75 + \frac{95.8188}{0.0030}\right) e^{0.0030t} - \frac{95.8188}{0.0030} \quad t = 1, 2, \dots, n$$

The state transition matrix is

$$\mathbf{P} = \begin{bmatrix} 0.8261 & 0.1739 & 0 & 0 & 0 \\ 0.0625 & 0.8625 & 0.0750 & 0 & 0 \\ 0 & 0.0769 & 0.9011 & 0.0220 & 0 \\ 0 & 0 & 0.0250 & 0.9500 & 0.0250 \\ 0 & 0 & 0 & 0.0800 & 0.9200 \end{bmatrix}$$

The residuals E_1, E_2, E_3, E_4, E_5 of five error states are divided according to 1-300 groups of data. The partition state of the residual range is shown in Table 5. By using the above formula, the predicted values of the vibration acceleration signal energy are obtained, and some of the data are shown in Table 6.

Table 5. Division of error status

Status	E_1	E_2	E_3	E_4	E_5
Residual error range	$[-10.4549 : -6.2492]$	$[-6.2492 : -2.0434]$	$[-2.0434 : 2.1623]$	$[2.1623 : 6.3681]$	$[6.3681 : 10.5738]$

Table 6. Grey-Markov model partial prediction results

Sample data	True value	Predicted value	Relative error
1	100.0061	100.0061	0.00%
2	100.7538	94.2241	6.48%
3	101.6388	98.7219	2.87%
4	102.1881	99.0149	3.11%
5	102.5543	99.3087	3.16%
\vdots	\vdots	\vdots	\vdots
298	226.3253	225.5419	0.35%
299	226.6507	226.2579	0.17%
300	226.9761	226.9761	0.00%

Figure 8 displays the comparison between the predicted and actual energy and values of each state of vibration acceleration signal predicted by the Grey-Markov model and the actual values.

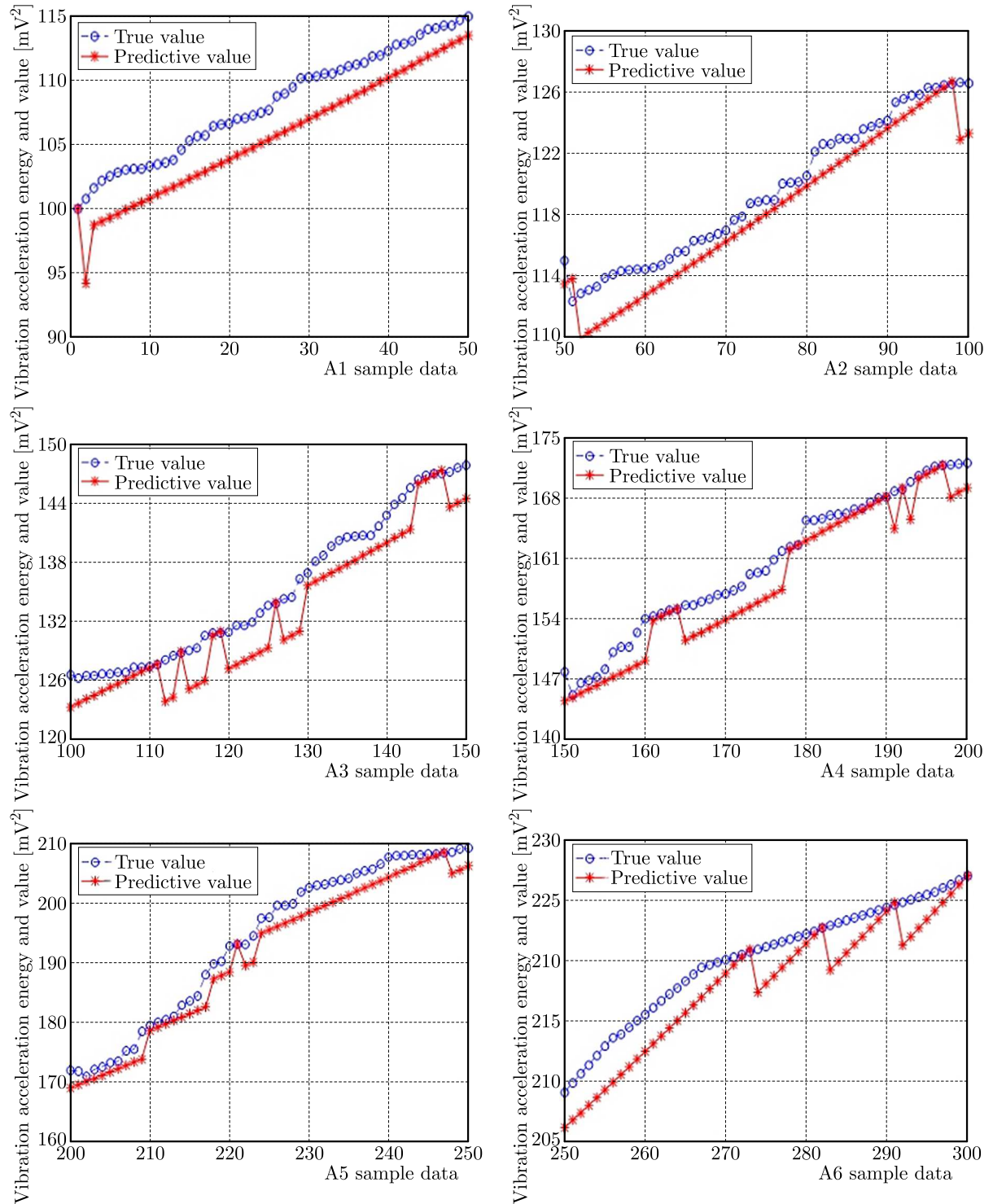


Fig. 8. Comparison diagrams of Grey-Markov real values and predicted values of the vibration signal

It is noted from Fig. 8 that the overall Grey-Markov model for each interval of the pick wear state data prediction is relatively accurate, when 1 to 50 group of data is taken as a reference

and the Grey-Markov model is used to predict such 250 groups of data, with an average relative error of 1.43%.

4.2. Acoustic emission signal prediction model

The energy and characteristic samples of acoustic emission signal are synthesized into characteristic directions $\mathbf{x}^{(0)}$

$$\mathbf{x}^{(1)} = [64.5960, 64.5881, 64.5314, 64.1547, \dots, 11.0485, 11.0112, 11.0043, 10.9641]$$

The matrix \mathbf{B} and vector \mathbf{Y}_n are obtained according to the Grey-Markov rule as follows

$$\mathbf{B} = \begin{bmatrix} -64.5921 & 1 \\ -64.5598 & 1 \\ -64.3431 & 1 \\ -64.1260 & 1 \\ \vdots & \vdots \\ -11.0855 & 1 \\ -11.0299 & 1 \\ -11.0078 & 1 \\ -10.9842 & 1 \end{bmatrix}$$

$$\mathbf{Y}_n = [64.5881, 64.5314, 64.1547, 64.0972, \dots, 11.0485, 11.0112, 11.0043, 10.9641]$$

$$\mathbf{x} = \begin{bmatrix} a \\ u \end{bmatrix} = (\mathbf{B}^T \mathbf{B})^{-1} \mathbf{B}^T \mathbf{Y} = \begin{bmatrix} 0.0054 \\ 65.4765 \end{bmatrix}$$

The solution

$$\hat{x}^{(1)}(t+1) = \left(64.5881 + \frac{65.4765}{0.0054}\right) e^{0.0054t} - \frac{65.4765}{0.0054} \quad t = 1, 2, \dots, n$$

The state transition matrix is

$$\mathbf{P} = \begin{bmatrix} 0.9744 & 0.0256 & 0 & 0 & 0 \\ 0.0435 & 0.7826 & 0.1739 & 0 & 0 \\ 0 & 0.0732 & 0.8455 & 0.0813 & 0 \\ 0 & 0 & 0.1515 & 0.7879 & 0.0606 \\ 0 & 0 & 0 & 0.1600 & 0.8400 \end{bmatrix}$$

The residuals E_1, E_2, E_3, E_4, E_5 of the five error states are divided according to 1-300 groups of data. The partition state of the residual range is shown in Table 7. The predicted values of energy and acoustic emission acceleration signal in the frequency domain obtained by using the above formula are shown in Table 8.

Table 7. Division of error status

Status	E_1	E_2	E_3	E_4	E_5
Residual error range	$[-2.4877 : -1.4916]$	$[-1.4916 : -0.4956]$	$[-0.4956 : 0.5004]$	$[0.5004 : 1.4964]$	$[1.4964 : 2.4924]$

From Fig. 9, it is evident that the average relative error of the prediction of the Grey-Markov model is 1.64%. The results show that the average relative error of the Grey-Markov model is marginal and acceptable for this sample size. The aforesaid predictions of each feature sample data based on the Grey-Markov model prove that the Grey-Markov model gives a small relative error and a high prediction accuracy.

Table 8. Grey-Markov model partial prediction results

Sample data	True value	Predicted value	Relative error
1	64.5960	64.5960	0.00%
2	64.5881	64.4557	0.20%
3	64.5314	64.1054	0.66%
⋮	⋮	⋮	⋮
298	11.0112	10.6160	3.59%
299	11.0043	10.5453	4.17%
300	10.9641	10.4750	4.46%

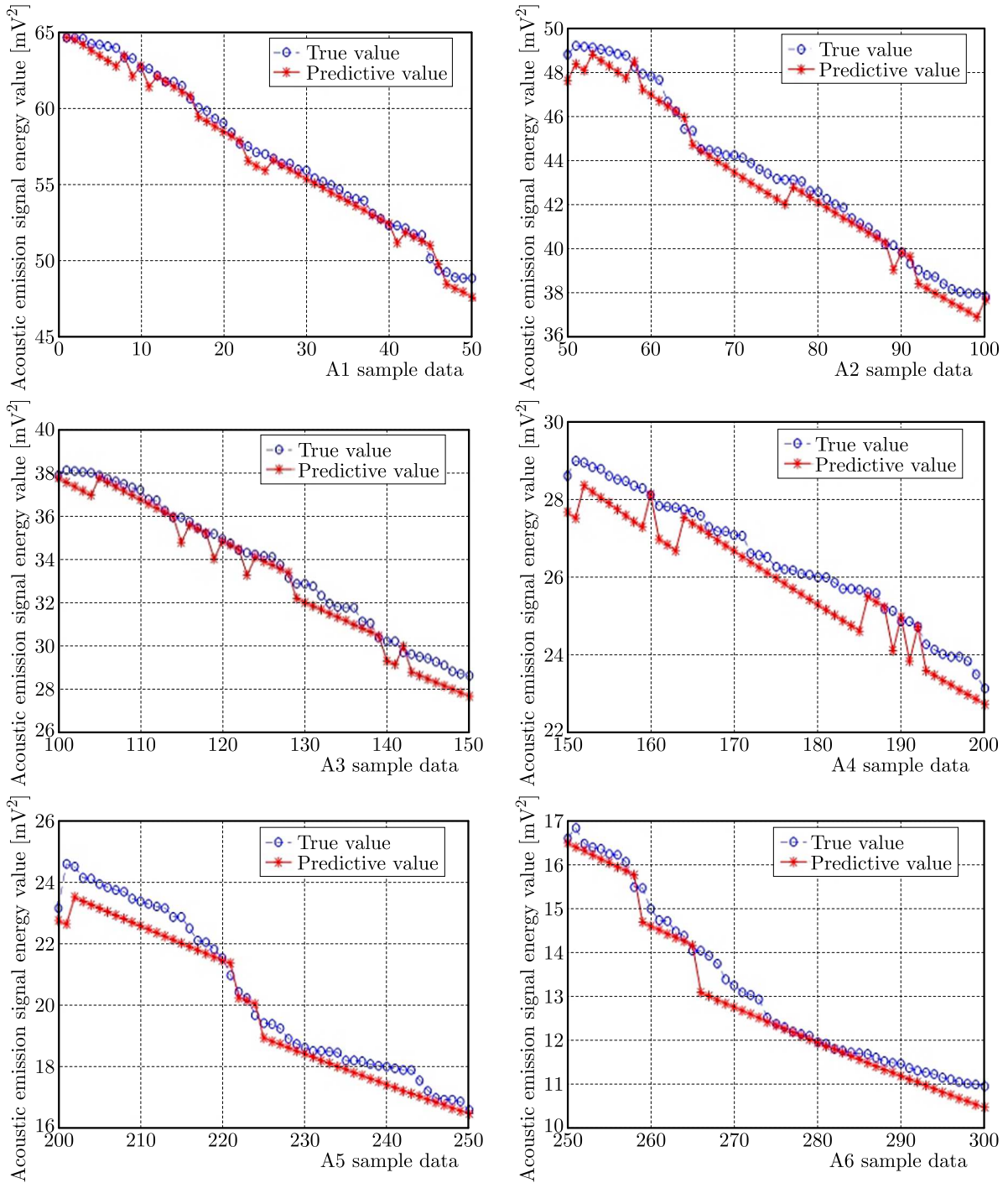


Fig. 9. Comparison of Grey Markov predicted values and real values of AE signal

5. Conclusion

- The characteristic signals of different wear picks in the pick process are obtained by pick experiments. With a change in the pick wear state, the peak value of the pick vibration acceleration in the time domain for six pick wear states increases continuously, whereas the peak value of the acoustic emission signal continuously decreases.
- The present Grey-Markov chain prediction model decides about picks in the cutting process based on characteristic signals and certain pick wear parameters of the data used in this model. The results show that the predictions based on the degree of vibration signal and the acoustic emission signal have an average relative error of 1.43% and 1.64%, respectively, indicating a high prediction accuracy for the state of the pick wear prediction.

Acknowledgment

The research was supported by the National Natural Science Foundation of China (51774161).

References

1. BAGRI S., MANWAR A, VARGHESE A., MUJUMDAR S., JOSHI S.S., 2021, Tool wear and remaining useful life prediction in micro-milling along complex tool paths using neural networks, *Journal of Manufacturing Processes*, **71**, 679-698
2. BOING D., CASTRO F.L., SCHROETER R.B., 2020, Prediction of PCBN tool life in hard turning process based on the three-dimensional tool wear parameter, *The International Journal of Advanced Manufacturing Technology*, **106**, 3, 779-790
3. CHEN J.J, WANG Y.F., ZHANG Y., YANG S.B., ZHANG X.Q., 2020, Investigation on tool wear mechanism during dry cutting 304 stainless steel, *CIRP Annals*, **20**, 1, 36-44
4. FAN Y.M., GHAYESH M.H., LU T.F., 2020, Enhanced nonlinear energy harvesting using combined primary and parametric resonances: Experiments with theoretical verifications, *Energy Conversion and Management*, **221**, 113061
5. HU M., MING W.W., AN Q.L., CHEN M., 2019, Tool wear monitoring in milling of titanium alloy Ti-6Al-4 V under MQL conditions based on a new tool wear categorization method, *The International Journal of Advanced Manufacturing Technology*, **104**, 4117-4128
6. LAN H., XIA Y. M., MIAO B., FU J., JI Z.Y., 2020, Prediction model of wear rate of inner disc cutter of engineering in Yinsong, Jilin, *Tunnelling and Underground Space Technology*, **99**, 103338
7. LI X.R., ZHU J.M., TIAN F.Q., PAN H.F., 2020, Discrimination and prediction of tool wear state based on Grey theory, *Journal of Testing and Evaluation*, **48**, 6, JTE20180302
8. LUBIS S., DARMAWAN S., ROSEHAN, WINATA W., ZULKARNAIN M., 2020, Tool wear analysis of ceramic cutting tools in the turning of gray cast iron materials, *IOP Conference Series: Materials Science and Engineering*, **857**, 012003
9. ŁUCZAK B., FIRLIK B., STAŚKIEWICZ T., SUMELKA W., 2022, Numerical algorithm for predicting wheel flange wear in trams – validation in a curved track, *Proceedings of the Institution of Mechanical Engineers, Part F: Journal of Rail and Rapid Transit*, **48**, 3, 751-770
10. MA Z., XU X.W., HUANG X.H., MING W.W., AN Q.L., CHEN M., 2022, Cutting performance and tool wear of SiAlON and TiC-whisker-reinforced Si₃N₄ ceramic tools in side milling Inconel 718, *Ceramics International*, **48**, 3, 3096-3108
11. OUAFIK Y., 2020, Numerical analysis of a frictional contact problem for thermo-electro-elastic materials, *Journal of Theoretical and Applied Mechanics*, **58**, 3, 673-683

12. SHADFAR M., MOLATEFI H., 2017, A study on transient wear behavior of new freight wheel profiles due to two point contact in contact in curve negotiation, *Journal of Theoretical and Applied Mechanics*, **55**, 2, 621-634
13. SHEN X., CHEN X.S., FU Y.B., CAO C.Y., YUAN D.J., LI X.H., XIAO Y.S., 2022, Prediction and analysis of slurry shield TBM disc cutter wear and its application in cutter change time, *Wear*, **498-499**, 204314

Manuscript received April 13, 2022; accepted for print December 10, 2022